ELSEVIER

Polymer 44 (2003) 2781–2791

polymer

www.elsevier.com/locate/polymer

Dielectric studies of molecular mobility in hybrid polyimide–poly(dimethylsiloxane) networks

S. Kripotou[a], P. Pissis[a,*], V.A. Bershtein[b], P. Sysel[c], R. Hobzova[c]

[a]*Department of Physics, National Technical University, Zografou Campus, 157 80 Athens, Greece*
[b]*Ioffe Physico-Technical Institute of the Russian Academy of Sciences, 26 Polytechnicheskaya Str., 194021 St Petersburg, Russia*
[c]*Departement of Polymers, Institute of Chemical Technology, Technicka 5, 16628 Prague 6, Czech Republic*

Received 23 October 2002; accepted 4 January 2003

Abstract

Dielectric techniques, including broadband dielectric relaxation spectroscopy and thermally stimulated depolarization currents, and to a lesser extent differential scanning calorimetry and equilibrium water sorption isotherm measurements, were employed to investigate molecular mobility in relation to morphology in polyimide–poly(dimethylsiloxane) hybrid networks (PI–PDMS). NMR measurements on the same samples had indicated that short PDMS chains with both ends chemically bound to the PI phase, form spherical domains of nanometer size. The local, secondary γ relaxation of PI, the primary α relaxation, associated to the glass transition of PDMS, and the interfacial Maxwell–Wagner–Sillars relaxation, related to the microphase-separated morphology, were studied in detail. The results are discussed in terms of nanoscale confinement of both components and of fixed chain ends of the PDMS component. These factors were found to affect considerably the magnitude of γ and the α relaxations, whereas the time scale of the relaxations remains practically unchanged.

Keywords: Hybrid networks; Molecular mobility; Dielectric techniques

1. Introduction

Polyimides (PIs) find many technological applications, in particular, in advanced microelectronics, aerospace and printed circuit industries due to their excellent thermal stability, mechanical and dielectric properties [1–4]. For some of these applications specific properties have to be improved by combination with a second component, often with polysiloxanes. The latter are characterized by low strength and modulus and low glass transition temperature, possess however many distinguished properties, such as oxidative stability, gas permeability and dielectric behavior [5,6]. In fact, several linear random or block PI–PDMS copolymers have been prepared by incorporation of suitably terminated flexible oligo(dimethylsiloxanes) in PI chains and characterized by various techniques [6–8]. They show higher solubility, impact strength and lower water uptake, as compared to pure PI, at the same time, however, also reduced thermal and chemical stability and tensile strength [7,8]. The overall stability can be improved by crosslinking the linear chains into a three-dimensional network [9].

In this paper we report the results of molecular mobility studies, mostly by dielectric techniques, in polyimide–poly(dimethylsiloxane) hybrid networks (PI–PDMS). The preparation of the samples has been described elsewhere [10], as well as a detailed investigation at 30 °C of dynamics and nanostructure by several solid-state NMR techniques [11]. The NMR results indicate that there is only small amount of free terminal units in PDMS chains in the prepared products, i.e. both ends of PDMS chains are chemically bound to the PI phase (end of PI chains). The PDMS chains form spherical domains, whose size, in the range of a few nanometers, increases with increasing weight fraction/chain length of PDMS.

With respect to molecular mobility, the NMR results indicated the existence of two fractions of PDMS chains: (a) a fraction of highly mobile sequences of monomer units located in the inner part of PDMS domains which increases from 27 to 83 mol% of the PDMS phase with increasing

* Corresponding author. Tel.: +30-10-7722986; fax: +30-10-7722932.
E-mail address: ppissis@central.ntua.gr (P. Pissis).

0032-3861/03/$ - see front matter © 2003 Elsevier Science Ltd. All rights reserved.
doi:10.1016/S0032-3861(03)00136-8

weight fraction/chain length of PDMS, and (b) a fraction of PDMS chain fragments partially immobilized by the intimate interaction with rigid PI chains; the latter prevailed in the hybrid network with 10% PDMS and short PDMS chains. Thus, NMR experiments [11] clearly detected heterogeneity of segmental dynamics in PDMS chains of hybrids.

In the present research the emphasis is put on the investigation of molecular mobility in PI–PDMS networks by combining two dielectric techniques, broadband dielectric relaxation spectroscopy (DRS) and thermally stimulated depolarization currents (TSDC). The primary α relaxation, associated to the glass transition, of the PDMS phase, the secondary γ relaxation of the PI phase and the interfacial Maxwell–Wagner–Sillars (MWS) relaxation, related to the morphology of the PI–PDMS systems, are investigated by the dielectric techniques. DRS allows to study these processes in detail by varying frequency and temperature [12]. On the other hand TSDC, which in terms of DRS, corresponds to measuring dielectric losses as a function of temperature at constant low frequencies around 10^{-3} Hz, is characterized by high sensitivity and high resolving power, thus rendering the technique particularly attractive for investigating complex, multicomponent systems [13]. In addition to dielectric techniques, differential scanning calorimetry (DSC) was employed in the present research to study the glass transition and crystallization-melting events in the PDMS phase. Finally, water uptake of the samples was studied in some detail, by recording equilibrium water sorption isotherms (ESI) and analyzing the data in terms of the Guggenheim–Anderson–de Boer (GAB) equation [14].

Besides their high technological significance, the materials under investigation are interesting also from the fundamental point of view, in particular with respect to the study of the dynamics of short PDMS chains (Table 1) fixed at both ends. Schroeder and Roland [15] investigated by DRS the segmental α relaxation of end-linked poly(dimethylsiloxane) (PDMS) networks with the molecular weight between crosslinks varying from $M_c = 62,700$ down to $M_c = 186$ and observed marked changes for M_c lower than about 1000. The main difference here, as compared to Ref. [15], is that the PDMS chains are chemically bound to more immobile and rigid PI chains. In that respect there is some similarity to the DRS study of the dynamics of short poly(oxybutylene) chains in block copolymers with poly(oxyethylene) at low temperatures, where the poly(oxyethylene) blocks are crystalline, whereas the poly(oxybutylene) blocks remain amorphous [16].

Table 1
The hybrid networks are investigated. All the characteristics refer to PDMS. w is the weight and v the volume fraction, M_n the number-average molecular weight [10], N the number of backbone bonds ($= M_n/37$) and $\langle r^2\rangle^{1/2}$ the root-mean-square end-to-end distance of unperturbed chain calculated from Eq. (1) [15]

Network	w (wt%)	v (vol%)	M_n (g/mol)	N	$\langle r^2\rangle^{1/2}$ (nm)
PI	0				
PI–PDMS 90/10	10	12.79	340	9	1.2
PI–PDMS 78/22	22	27.12	950	26	2.1
PI–PDMS 70/30	30	36.12	1480	40	2.6
PI–PDMS 69/31	31	37.22	1500	41	2.7

2. Experimental

The materials were prepared from poly(amic acid) based on 4,4′-oxydiphthalic anhydride and 4,4′-oxydianiline and terminated by 4-aminophenyltrimethoxysilane. Dimethoxydimethylsilane, a precursor of PDMS, was used to form PDMS crosslinks between PI chains (Fig. 1). The final networks were prepared by thermal exposition of a thin layer of a mixture of PI and PDMS precursors on a glass or teflon substrate. Four networks with varying weight fraction of PDMS were prepared and investigated. Details of the preparation of the samples have been given elsewhere [10]. Some characteristics of the samples referring to PDMS are listed in Table 1. The weight fraction w and the molecular weight M_n have been estimated in Ref. [10]. For calculating the volume fraction v densities $\rho = 1.28$ and 0.97 g/cm^3 have been used for PI and PDMS, respectively, [11]. The root-mean-square end-to-end distance in the unperturbed state of chain $\langle r^2\rangle^{1/2}$ has been calculated from

$$\langle r^2\rangle = N\ell^2 C_n \tag{1}$$

with values for the bond length $\ell = 0.164$ nm and the characteristic ratio $C_n = 6.43$ taken from Ref. [15]. This value characterizes only approximately the end-to-end distance for PDMS chains as crosslinks in the hybrid

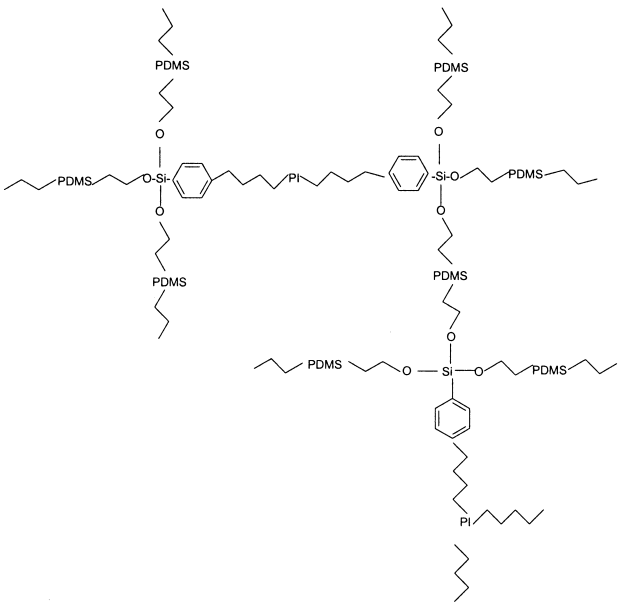

Fig. 1. PI–PDMS network.

networks under study and varied from ~1.2 to 2.7 nm (Table 1).

DSC measurements were performed using the Perkin–Elmer DSC-2 apparatus, in the temperature range from 100 to 300 K in nitrogen atmosphere.

For DRS measurements the complex dielectric permittivity, $\varepsilon^* = \varepsilon' - i\varepsilon''$, was determined as a function of frequency (10^{-2}–10^6 Hz) in the temperature range from 130 to 350 K (controlled to better than ±0.1 K). A Schlumberger Frequency Response Analyzer (FRA SI 1260) supplemented by a buffer amplifier of variable gain (Chelsea Dielectric Interface) in combination with the Novocontrol Quatro Cryosystem were used. The samples were circular films of 20 mm diameter and thickness between 100 and 250 μm.

The TSDC measurements were performed at circular films with 14 mm in diameter. The sample was inserted between the brass plates of a capacitor and polarized by the application of electric field E_p at temperature T_p for time t_p, which was large in comparison with the relaxation time at T_p of the dielectric dispersion under investigation. With the electric field still applied, the sample was cooled to temperature T_0 (which was sufficiently low to prevent depolarization by thermal excitation), and then was short-circuited and reheated at a constant rate b. A discharge current was generated as a function of temperature, which was measured with a sensitive electrometer. The equivalent frequency f of TSDC measurements [13] spans $10^{-4} < f < 10^{-2}$ Hz, i.e. it is close to those of DSC measurements. High TSDC sensitivity allows the detection of weak relaxations.

A homemade experimental apparatus for TSDC measurements was used, which operated over the temperature range from 77 to 300 K [13]. Typical conditions were $E_p = 6$ kV/cm for the polarizing field, $T_p = 300$ K for the polarization temperature, $t_p = 5$ min for the polarization time, 6 K/min for the cooling rate to $T_0 = 88$ K, and $b = 3$ K/min for the heating rate.

ESI were measured at 25 °C. The samples were allowed to equilibrate to constant weight (until the sample weight change was less than 10^{-4} g) in various desiccators where the RH was kept constant between 0.06 and 0.97 using various saturated salt solutions [17]. The water content, h, defined as the ratio of the weight of water to the weight of the dry sample, was determined by weighing.

3. Results and discussion

3.1. DSC measurements

Fig. 2 shows DSC thermograms obtained at a heating rate of 10 K/min, after cooling from 290 to 100 K at a cooling rate of 320 K/min. The results obtained for the four hybrid networks are compared with those in linear PDMS with number-average molecular weight $M_n = 7400$ [18] and in crosslinked PDMS with molecular weight between cross-

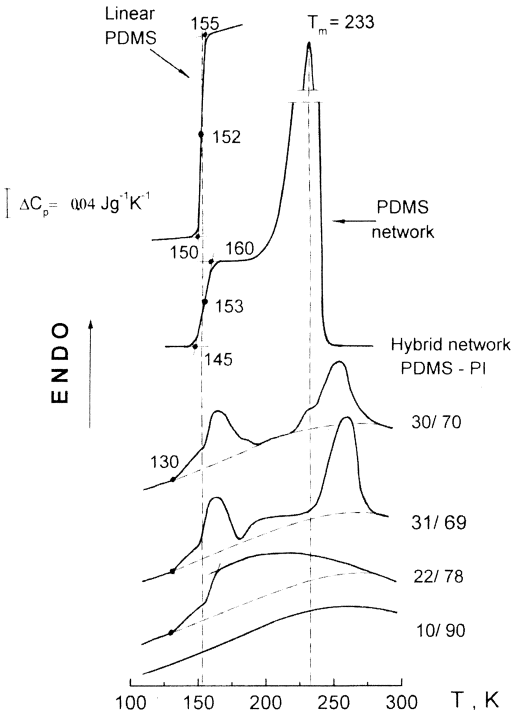

Fig. 2. DSC thermograms at a heating rate of 10 K/min for the samples indicated on the plot.

links $M_c = 17,300$. DSC measurements at higher temperatures (not shown here) give for the glass transition temperature T_g of the PI component values in the range 525–534 K. They are in the same range as those reported for the same samples earlier (528–542 K) and lower than $T_g = 563$ K obtained for pure PI [11]. In polysiloxane-*block*-polyimides T_g of PI was found to decrease significantly with increasing PDMS content [6]. Significant changes in the glass transition behavior of the PI component were also observed in alternating phase-separated PI–PDMS block copolymers [18]. These results suggest a different behavior of the PI–PDMS networks, as compared to the PI/PDMS block copolymers, as also indicated in Ref. [11] on the basis of mechanical data.

With respect to the PDMS component, Fig. 2 indicates very special behavior of the hybrid networks, as compared to pure PDMS. A broadening is observed in the glass transition range in the hybrid networks, which is about 30 K (from 130 to 160 K) in PI–PDMS 70:30, as compared to 5 K (from 150 to 155 K) in linear PDMS and 15 K (from 145 to 160 K) in the pure PDMS network. This behavior is in qualitative agreement with dynamic heterogeneities observed by NMR in the PDMS phase of the hybrid networks under investigation [11] and can be explained on the basis of two opposite effects [18,19]: (a) nanoscale confinement resulting in loosening of PDMS segmental packing and collapsing of intermolecular cooperativity of PDMS segmental motion, so that T_g of about 150 K is displaced to the temperature of non-cooperative β relaxation, $T_\beta \sim 130$ K [18], and (b) some constraining influence

of the rigid PI component on PDMS segmental motion leading to some increasing of the glass transition completion temperature and immobilization of PDMS chains. Effect (a) is consistent with the nanometer size of the PDMS domains in the hybrid networks determined in Ref. [11]. With respect to the suppression of cooperative segmental motion in PDMS nanodomains, it is interesting to note that DSC measurements showed a substantial decrease in the heat capacity jump at T_g of PDMS layers grafted onto silica surfaces [20].

At temperatures higher than T_g of PDMS, the endothermic peak on the DSC curve of the PDMS network corresponds to melting of slightly crystallized sample. No such peak was observed for the linear PDMS studied. In contrast to pure PDMS samples, a small exothermic effect of some ordering of mesophase type (which sharply differs from much more intense and narrow exotherm in usual PDMS crystallization), following directly the glass transition completion (i.e. the temperature of completion of the heat capacity step on the DSC curve), is observed in the range of ~160–220 K in the hybrid networks with the highest PDMS content, 30 and 31 wt%, in Fig. 2. M_n for these samples is about 1500, corresponding to about 20 monomer units, i.e. about 4–5 Kuhn statistical segments. For these two networks an endothermic effect is observed in the temperature region ~230 to ~280 K and only some trace of real melting peak ($T_m = 233$ K). The short length of PDMS chains and their anchoring from both ends to rigid PI constraints prevents, obviously, the formation of real PDMS crystallites, which were observed in the pure PDMS network. Thus, it may be assumed that the endotherm in the region 230–280 K is associated with some kind of 'constrained melting' of the mesophase state which is formed in the PDMS component due to the influence of PI.

In the case of the network with 22 wt% PDMS, $M_n = 950$, corresponding to about 13 monomer units or 3 Kuhn statistical segments, the ability of grafted PDMS to ordering and formation of crystalline nuclei or mesophase is lost and only the extended and complex heat capacity step in the glass transition region is observed in the DSC thermogram. It is interesting to note in this connection that DSC measurements showed that crystallinity is suppressed in PDMS layers grafted onto silica surfaces [20] and the same was also observed in PDMS filled with hydrophilic and hydrophobic Aerosil [21]. Finally, for the hybrid network with the lowest PDMS content of 10 wt% and PDMS chains with $M_n = 340$, corresponding to 5 monomer units or 1 Kuhn segment only, total suppression of segmental rearrangements including glass transition is observed in Fig. 2. We come back to this point later, in connection with the high-sensitivity TSDC measurements.

These DSC data are in a qualitative accordance with the abovementioned NMR data [11]. In the ^{29}Si NMR spectrum of the PI–PDMS network with 10 wt% PDMS only a weak signal was observed. Short PDMS chains (crosslinks) with ca. 5 monomer units were formed in that case. Because of hindered molecular motion and various local magnetic environments, their NMR signals were inhomogeneously broadened and, thus, very weak. On the contrary, highly mobile dimethylsiloxane sequences were observed in PDMS chains (crosslinks) with the number of monomer units $n > 10$.

3.2. The overall dielectric response

The TSDC technique allows for a quick characterization of the various relaxation processes contributing to the dielectric response of the sample under investigation. Fig. 3 shows TSDC thermograms obtained with pure PI and the four hybrid networks. With respect to the more conventional DRS measurements to be reported later, the TSDC plot corresponds to measuring dielectric losses as a function of temperature at fixed low frequencies in the range 10^{-2}–10^{-4} Hz. Two dispersion regions are observed in Fig. 3, the first at low temperatures in the region 140–170 K and the second, not present in pure PI, at higher temperatures in the region 180–220 K.

In pure PI the low-temperature dispersion consists of a single, weak relaxation centered at $T_\gamma = 145$ K (inset to Fig. 3). This is the secondary γ relaxation, studied in some detail for the same PI and other PIs in Ref. [19,22]. Detailed measurements reported there, including the measurements on poly(amide–imide)s, have indicated that this relaxation, which is also mechanically active with activation parameters similar to those obtained by dielectric measurements, must be attributed to non-cooperative torsion vibrations of imide cycles. In the hybrids the γ relaxation is masked by a new relaxation, which appears at about 155–160 K (Table 2) and increases in magnitude with increasing amount of PDMS. This new relaxation is the primary (segmental) α relaxation associated with the glass transition in the PDMS domains, in consistency with the results of DSC measurements in Fig. 2 and in Ref. [11], bearing in mind that DSC and TSDC are characterized by similar equivalent frequencies in the range 10^{-2}–10^{-4} Hz [23].

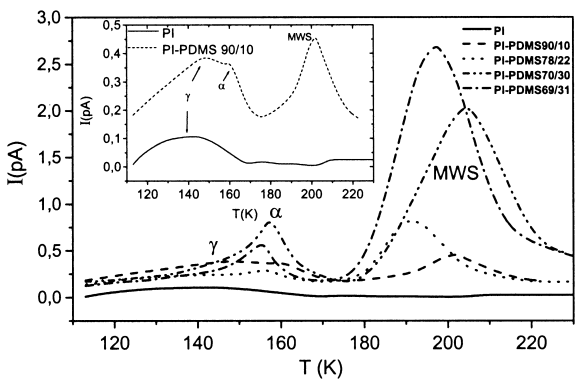

Fig. 3. TSDC thermograms obtained with the hybrid networks indicated on the plot. The inset shows details of the thermograms for pure PI and PI–PDMS 90/10.

Table 2
Results of the analysis of TSDC measurements. T_α and T_{MWS} are the peak temperatures of the α relaxation of PDMS and of interfacial MWS relaxation respectively. $\Delta\varepsilon_\alpha$ and $\Delta\varepsilon_{MWS}$ are the corresponding relaxation strengths. The apparent activation energy E_{act} and the pre-exponential factor τ_0 refer to the MWS relaxation

Network	T_α (K)	T_{MWS} (K)	$\Delta\varepsilon_\alpha$	$\Delta\varepsilon_{MWS}$	E_{act} (eV)	τ_0 (s)
PI–PDMS 90/10	160	202	0.03	0.07	0.59	2.3×10^{-13}
PI–PDMS 78/22	157	191	0.03	0.20	0.49	1.5×10^{-11}
PI–PDMS 70/30	157	203	0.13	0.39	0.36	2.3×10^{-7}
PI–PDMS 69/31	156	196	0.10	0.48	0.46	2.1×10^{-10}

The high-temperature TSDC peak in the region 180–220 K in Fig. 3 is attributed to the interfacial MWS relaxation. This relaxation is characteristic for heterogeneous systems with different conductivities of the two phases, like the PDMS inclusions and the PI matrix in the hybrid networks under investigation here. The MWS polarization arises then from the accumulation of charges at the PDMS–PI interfaces during the polarization step, which gives rise to the TSDC MWS peak in the depolarization step. The main arguments for assigning the high-temperature TSDC peak to the MWS relaxation, at this stage, is that (a) the peak is located at temperatures higher than T_g of PDMS, which forms isolated domains in a glassy, i.e. less conductive PI matrix, and (b) the peak is not present in pure PI.

As a counterpart to the TSDC plot in Fig. 3, Fig. 4 shows the overall DRS response of pure PI and three hybrid networks at 303 K. The response of the network with 30 wt% PDMS is very similar to that of the sample with 31 wt% PDMS and has been omitted here for clarity. Two dispersions are observed in Fig. 4: the γ relaxation of PI at high frequencies, present in all the samples studied, and the more intense MWS relaxation at lower frequencies, present only in the hybrid networks. The MWS relaxation shifts to lower frequencies (becomes slower) with increasing PDMS content and becomes more intense.

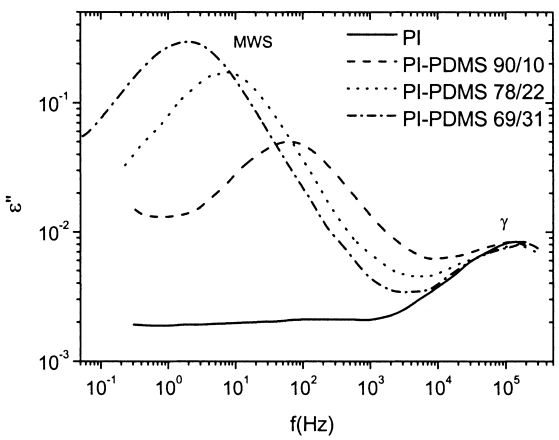

Fig. 4. Dielectric loss ε'' versus frequency f at 303 K for the samples indicated on the plot.

The α relaxation of PDMS, which overlaps with γ of PI in the TSDC thermograms of Fig. 3 in the temperature region of 140–160 K, is not observed in Fig. 4. That is because the two relaxations are characterized by quite different temperature dependence. The α relaxation shifts with temperature are much faster than the γ relaxation of PI and at 303 K is out of the frequency range of measurements in Fig. 4. To complete these introductory remarks on the overall dielectric response of the samples under investigation, Fig. 5 shows $\varepsilon''(f)$ in the sample with the highest PDMS content (31 wt%) at low temperatures, where the α relaxation of PDMS can be followed.

In the following we present the DRS and TSDC characteristics of the three relaxations studied, γ, α and MWS, and discuss their implications.

3.3. The γ relaxation of PI

Fig. 6 shows the isochronal (constant frequency) plot of $\varepsilon''(T)$ in the region of the γ relaxation of PI for pure PI and the hybrid networks with 10 and 31 wt% of PDMS. The data have been recorded isothermally as a function of frequency and have been replotted here, one reason for that being to allow comparison with the TSDC data in Fig. 3. As indicated in Fig. 3 (and more clearly in the inset to Fig. 3), the γ relaxation of PI increases in magnitude by addition of 10 wt% PDMS and shifts slightly to higher temperatures ($T_\gamma = 145$ K in pure PI against $T_\gamma = 148$ K in the hybrid with 10 wt% PDMS), i.e. it becomes slightly slower in the hybrid networks. The relaxation strength $\Delta\varepsilon$, calculated from the equation [13]

$$\Delta\varepsilon = \frac{Q}{A\varepsilon_0 E_p} \tag{2}$$

where A is the cross sectional area of the sample, ε_0 the permitivity of free space, E_p the polarizing field and Q the depolarization charge, obtained from the area under the depolarization current peak, increases from $\Delta\varepsilon = 0.06$ for

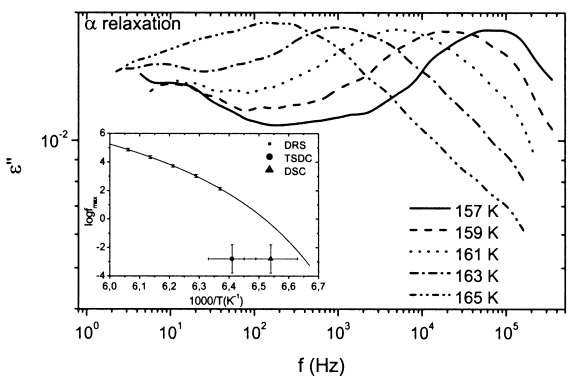

Fig. 5. Dielectric loss ε'' versus frequency f in PI–PDMS 69/31 at several temperatures in the region of α relaxation of PDMS. The inset shows the Arrhenius plot. The line is a fit of the VTF equation (Eq. (5)) to the DRS data.

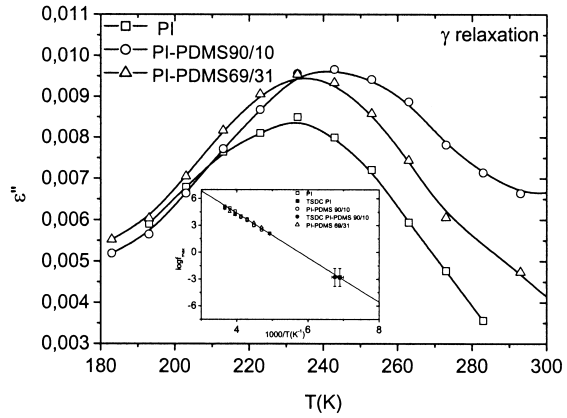

Fig. 6. Isochronal (constant frequency, $f = 5 \times 10^3$ Hz) plot of dielectric loss ε'' versus temperature T in the region of the γ relaxation of PI for the samples indicated on the plot. The inset shows the Arrhenius plot for the γ relaxation.

pure PI to $\Delta\varepsilon = 0.10$ for the hybrid network with 10 wt% of PDMS. $\Delta\varepsilon$ could not be reliably determined for the other hybrid networks from the TSDC thermograms and Eq. (2), because of the strong overlapping with the α relaxation of PDMS. Thus, the local dynamics of PI is modified in the hybrid networks. This is more clearly shown in Fig. 6, where there is now no contribution from the α relaxation of PDMS. Please note that the magnitude of the relaxation increases in the hybrid networks with increasing PDMS content, although the amount of PI, which is responsible for the γ relaxation, decreases.

The kinetic parameters of the γ relaxation have been obtained by fitting the Arrhenius equation

$$f_{\max}(T) = f_0 \exp\left(-\frac{E_{\text{act}}}{kT}\right) \tag{3}$$

to the data. In this equation, which is characteristic for local, secondary relaxations in polymers, $f_{\max}$ is the frequency of $\varepsilon''(f)$ peak, T the temperature, f_0 a constant, E_{act} the apparent activation energy of the relaxation and k Boltzmann's constant. The inset to Fig. 6 shows the Arrhenius plot for the γ relaxation for the various samples studied. The TSDC points have been included for the two samples where T_γ could be reliably determined, $T_\gamma = 145$ K for PI and $T_\gamma = 148$ K for PI–PDMS 90/10, at the equivalent frequency of 1.6 MHz, corresponding to a relaxation time of 100 s [13,23]. In the samples with higher amount of PDMS the γ relaxation is masked by the α relaxation of PDMS (Fig. 3). The TSDC points are in excellent agreement with the DRS data, providing support that the DRS and the TSDC data refer to the same molecular mechanism and that the kinetic parameters, characteristic for that mechanism, do not change with temperature in the temperature range of DRS and TSDC measurements. For clarity error bars are shown only for the TSDC points ($\Delta T = \pm 2$ K, $\Delta \log f_{\max} = \pm 1$). The errors for the DRS data are: $\Delta \log f_{\max} = \pm 0.1$ and $\Delta T = \pm 0.1$ K. The straight line in the inset to Fig. 6 is that for pure PI, by also considering the TSDC point. E_{act} and f_0 are then determined to 0.49 eV (47 kJ/mol) and 2×10^{14} Hz, respectively. Within experimental errors (± 0.03 eV in E_{act} and about one order of magnitude in f_0), similar values have been also obtained in the hybrid networks, despite the slight shift to lower frequencies/higher temperatures. These values are in the range of E_{act} and f_0 values reported for the γ relaxation in various PIs [19,22]. The relatively high value of activation energy (with respect to the temperature/frequency range of the loss peak) is explained by the bulky shape of the imide cycles responsible for the γ relaxation. Normalized $\varepsilon''/\varepsilon''_{\max}(f/f_{\max})$ plots, not shown here, suggest that also the shape of the response, indicative of intermolecular interactions, does not practically change with the composition.

Thus, both DRS and TSDC data show that the magnitude of the γ relaxation of PI increases in the hybrid networks. The same data also suggest that the relaxation becomes slightly slower in the networks, as compared to pure PI. In searching for an explanation for this behavior it is interesting to compare the data obtained here with those obtained in similar systems. TSDC and DRS measurements in PI/silica nanocomposites showed that the γ relaxation of PI increases significantly in magnitude with increasing filler content, whereas the time scale of the relaxation does not practically change with composition [19,24]. It is interesting to note in this connection that water uptake in PI (and PI/silica nanocomposites) was found to have the same effect on the γ relaxation of PI, i.e. to increase the magnitude of the relaxation (and, in addition, to cause a slight shift to lower temperatures) [19]. These results have been discussed in terms of an overall enhancement of small-scale molecular mobility by incorporation of silica nanodomains in PI, arising from loosened molecular packing of PI chains, as compared to pure PI. We think that we are dealing with a similar situation in the PI–PDMS networks, if we consider the increase in the magnitude of the γ relaxation as the main effect.

In fact it may be assumed priori that such loosening originates from some steric hindrances to dense molecular packing of PI for two reasons: (a) the formation of chemical bonds between the PI chains and the PDMS chains, and (b) the confinement of PI in small volumes between the PDMS nanodomains. With respect to confinement, it is interesting to ask about the size of the corresponding volumes, i.e. about the mean distance R between PDMS nanodomains. R can be calculated from the equation [25]

$$R = d\left[\left(\frac{F}{v}\right)^{1/3} - 1\right] \tag{4}$$

where d is the size (diameter) of the domains, v the volume fraction of PDMS and F the PDMS packing factor. In this simple geometrical expression, commonly used for particulate composites, such as metal-filled polymers, the packing factor F defines the maximal possible filler content in the volume of polymer matrix. With $F = 0.64$ (for statistically

packed monodispersed spherical particles of any size) and the values of d determined for the PI–PDMS networks under investigation in Ref. [11], $d = 4.4$ nm in PI–PDMS 90/10 and $d = 11.2$ nm in PI–PDMS 78/22, R is calculated to 3.1 nm in the first network and to 3.7 nm in the second. Thus, the PI chains are located ('confined') in nanometer scale volumes between PDMS domains.

However, it is a very special case of nanoscale confinement, when the rigid polymer is confined by soft material. Therefore, the role of this second factor is not understood in prior. In fact, solid-state NMR studies in the hybrid networks under investigation here have indicated that the mobility of PI chains is not affected by the presence of the mobile PDMS component [11]. This result is more or less confirmed here by DRS and TSDC with respect to the time scale of the γ relaxation, however not with respect to its magnitude. By comparing mobility results obtained by various techniques, it should be beared in mind that, besides the extrinsic parameter of time scale, which may be different, the intrinsic parameter of spatial scale may also be different, as different techniques probe in general, the mobility of molecular units of different size. So, the γ relaxation studied by dielectric techniques here is attributed to local small-scale, non-cooperative motion of imide cycles, whereas NMR technique in the experiments [11] follows up segmental dynamics.

3.4. The α relaxation of PDMS

The most interesting result with respect to the α relaxation of PDMS in Fig. 3 is that this relaxation appears as a small shoulder on the high-temperature side of the γ relaxation of PI already in the hybrid with 10 wt% PDMS. The temperature position of the relaxation T_m does not practically change with composition and is very close to T_g determined by DSC in Fig. 2 and in Ref. [11]. The relaxation strength $\Delta\varepsilon_\alpha$, calculated from Eq. (2), becomes significant only for the hybrids with 30 and 31 wt% PDMS (Table 2). This explains why the glass transition of PDMS is not detected by DSC in the hybrid network with 10 wt% PDMS in Fig. 2 and in Ref. [11]. It is interesting to note in this connection that dynamic mechanical analysis measurements in polysiloxane-*block*-polyimides detect the mechanical α relaxation of PDMS at 15 wt% PDMS [6].

The dynamics of the α relaxation was studied by DRS only for the network with the highest amount of PDMS, 31 wt% (Fig. 5). The relaxation strength $\Delta\varepsilon_\alpha$ obtained from the DRS data (step in $\varepsilon'(f)$) is 0.10, in excellent agreement with that calculated from the TSDC data (Table 2). The inset to Fig. 5 shows the Arrhenius plot for the α relaxation. The Vogel–Tammann–Fulcher (VTF) equation [26]

$$f_{max} = A \exp\left(-\frac{B}{T - T_0}\right) \quad (5)$$

where A, B and T_0 (Vogel temperature) are temperature independent empirical parameters, was fitted to the DRS data and the fitting parameters were determined to log × $A = 11.0$, $B = 410$ K and $T_0 = 138$ K. T_g by DSC (153 K, Fig. 2) and T_α by TSDC (156 K, Table 2) have been included in the plot, both at the equivalent frequency of 1.6 MHz, corresponding to a relaxation time of 100 s [13]. Extrapolation of the VTF fit to this relaxation time gives $T_{g,diel}$ (defined by $\tau(T_{g,diel}) = 100$ s) equal to 150 K. Thus, $T_{g,diel}$ is lower than T_g and T_α by 3 and 6 K, respectively, i.e. by more than the experimental errors, included in the figure for T_g and T_α. It should be considered, however, that drastic extrapolation was necessary for the determination of $T_{g,diel}$. Under certain conditions, it is possible to give better estimates for the equivalent frequency of DSC and TSDC measurements, based on experimental data, and discuss more reliably, on that basis, the correlation of DRS and TSDC estimates of the glass transition temperature to T_g [23]. It is interesting to compare the dynamics of the α relaxation of PDMS in the hybrid networks to that in amorphous end-linked PDMS networks with systematically varying molecular weight M_c between crosslinks [15]. The dynamics was found to slow down with decreasing M_c and a similar trend may also be observed in the T_α data in Table 2. For comparable values of M_c the time-scale of the relaxation is very similar in the two systems. The fitting parameters log A, B and T_0 were also found to change systematically with M_c in Ref. [15] and the values obtained here for the hybrid network with 31 wt% PDMS fit well into the trend observed there.

The dependence of $\Delta\varepsilon_\alpha$ on composition in Table 2 indicates that a fraction of PDMS in the hybrid networks is immobilized with respect to the α relaxation (the glass transition), in qualitative agreement with the DSC data in Fig. 2. A further result can be added to that now, namely that the dynamics of the α relaxation of the mobile PDMS phase in the hybrid networks is very similar to that of bulk PDMS networks at comparable size of the PDMS chains [15]. The NMR results on the same hybrid networks showed that the amount of immobilized PDMS is nearly the same for all the compositions studied, as the size of the spherical domains formed by PDMS increases with increasing weight fraction/chain length of PDMS. Thus, the magnitude of the TSDC α relaxation (and the heat capacity jump at T_g in the DSC measurements) is significantly reduced in the hybrid networks with small PDMS content/short chains. The reason for that is not the small size of the domains, as compared to the cooperativity length of the glass transition, but the short length of the chains, which are fixed at both ends. It is interesting to note in this connection that, for the sample with 10 wt% PDMS, no glass transition was detected by DSC in Ref. [11] and in the present work, although the size of the PDMS nanodomains was determined to 4.4 nm for that composition (and that of the mobile phase to 3.2 nm), i.e. larger than the cooperativity length of the glass transition of PDMS of about 1.4 nm. Obviously, the terms mobile and immobilized phase always refer to a

specific mode of motion and values calculated for these phases depend on the experimental technique employed to probe mobility. Finally it is interesting to note that broadband DRS measurements in PDMS absorbed in Aerosil show three relaxation processes which were assigned to directly bound, interfacial and no PDMS is adsorbed [21].

3.5. The interfacial MWS relaxation

The TSDC results for the interfacial MWS relaxation, related to the heterogeneous structure of the hybrid networks, are presented in Fig. 3 and in Table 2. The peak temperature T_{MWS} does not change systematically with the composition, whereas the relaxation strength $\Delta\varepsilon$, calculated by Eq. (2), increases with increasing PDMS content. The values of $\Delta\varepsilon$ are rather high, providing support, that the relaxation is of the interfacial type [27]. The apparent activation energy E_{act} of the relaxation was calculated by the approximate half-width expression [28]

$$E_{act} = \frac{T_1 T_2}{4738(T_2 - T_1)} \tag{6}$$

where T_1 and T_2 denote the temperature at which the current drops is half its maximum value on the low-temperature and high-temperature sides, respectively. This equation has been derived for first-order peaks of thermally activated processes, such as thermoluminescence and TSDC, on the basis of the geometrical shape of the peak [28]. In Eq. (6) E_{act} and T are given in kJ mol^{-1} and K, respectively, and the factor 4738 is just a combination of constants and units [28]. The corresponding pre-exponential factor τ_0 in the Arrhenius equation for the relaxation time τ was calculated by

$$\tau_0 = \frac{kT_m^2}{bE_{act}} \exp\left[-\frac{E_{act}}{kT_m}\right] \tag{7}$$

where k is Boltzmann's constant, b the heating rate and T_m the peak temperature of the TSDC peak. The physical meaning of E_{act} is that it gives the activation energy of conductivity in the PDMS inclusions. E_{act} and τ_0 in Table 2 do not change systematically with composition. We will comment further on that point later.

In the comparative DRS measurements at 300 K in Fig. 4 the MWS loss peak was found to systematically shift to lower frequencies and to increase in magnitude with increasing PDMS content. The relaxation was further studied as a function of temperature. As an example, Fig. 7 shows the frequency dependence of dielectric permittivity and of dielectric loss ε'' at several temperatures. The Havriliak–Negami (HN) function [29]

$$\varepsilon^*(f) = \varepsilon_\infty + \frac{\Delta\varepsilon}{\left[1 + \left(\frac{if}{f_{HN}}\right)^{1-\alpha}\right]^\beta} \tag{8}$$

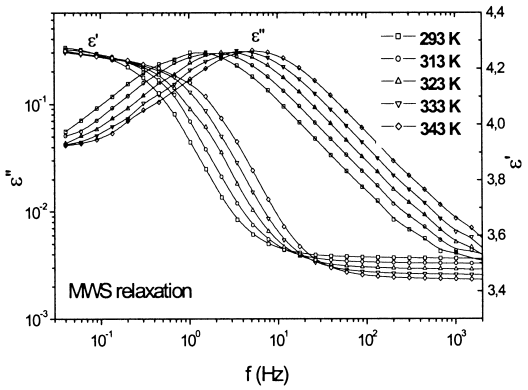

Fig. 7. Dielectric permittivity ε' and dielectric loss ε'' versus frequency f for PI–PDMS 69/31 in the region of the MWS relaxation at several temperatures indicated on the plot. The lines are to guide the eyes.

was fitted to the $\varepsilon'(f)$ and $\varepsilon''(f)$ ($\varepsilon^* = \varepsilon' - i\varepsilon''$) at each temperature and the characteristic frequency f_{HN}, the relaxation strength $\Delta\varepsilon$ and the shape parameters α and β were determined. ε_∞ in Eq. (8) is $\varepsilon'(f)$ for $f \gg f_{HN}$. The results of the analysis show that in each of the three hybrids studied (PDMS content 10, 22 and 31 wt%) $\beta = 1$ at each temperature, i.e. the loss peak is symmetric (which also means that the characteristic frequency f_{HN} is equal to the frequency f_{max} of maximum loss), and the values of α and $\Delta\varepsilon$ do not change much with temperature. These results provide further support that the relaxation under investigation is of the MWS type [27,30]. Table 3 lists values of f_{HN}, $\Delta\varepsilon$, α and β for the three systems studied at 303 K. The deviation from the Debye behavior ($\beta = 1$, $\alpha = 0$) is not very significant.

The loss peak frequencies f_{HN}, obtained at each temperature by Eq. (8) were used to construct the Arrhenius plot of the MWS relaxation shown in Fig. 8. For each network the data were fitted by the Arrhenius equation

$$f_{HN} = f_0 \exp\left(-\frac{E_{act}}{kT}\right) \tag{9}$$

and the values of the apparent activation energy E_{act} and the frequency factor f_0 are listed in Table 3.

It is striking that the DRS and the TSDC data for the MWS relaxation do not agree with each other, which was the case for the other two relaxations studied. This is due to the fact that the MWS relaxation reflects properties of the morphology, which is different in the temperature region of the TSDC MWS peak (around

Table 3
Values of the fitting parameters of Eqs. (8) and (9) for the MWS relaxation in the hybrid networks studied by DRS

Network	f_{HN} (Hz)	$\Delta\varepsilon$	α	β	E_{act} (eV)	f_0 (Hz)
PI–PDMS 90/10	58	0.14	0.21	1.0	0.24	6×10^5
PI–PDMS 78/22	6.6	0.43	0.14	1.0	0.31	9×10^5
PI–PDMS 69/31	1.7	0.79	0.17	1.0	0.31	3×10^5

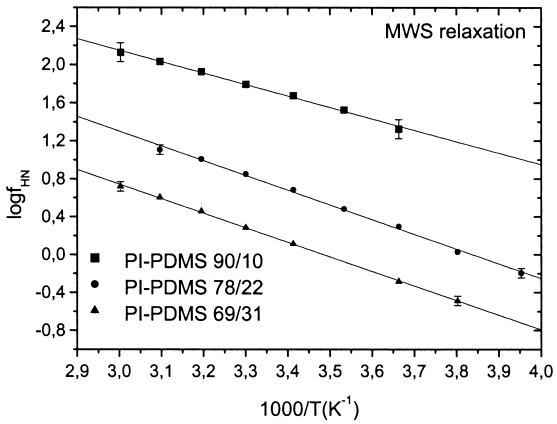

Fig. 8. Arrhenius plot of the MWS relaxation for the samples indicated on the plot.

200 K, Table 2), as compared to that in the temperature region of DRS measurements (293–343 K, Fig. 7). This situation is often faced in comparing DRS and TSDC results with each other and is due to the different frequency/temperature region of measurements by the two techniques: the equivalent frequency of TSDC measurements is in the range of 10^{-2}–10^{-4} Hz [13], which is typically out of or the lower limit of DRS measurements. As a result of that, TSDC peaks are typically at lower temperatures than the corresponding DRS loss peaks. In the region of DRS measurements PDMS is amorphous and, thus, E_{act} in Table 3 is the activation energy of conductivity in the amorphous PDMS nanophase. In the region of the TSDC MWS peak, i.e. around 200 K (Fig. 3), some ordering exists in the PDMS nanodomains, as indicated by the DSC data discussed in Section 3.1. This explains the higher values of activation energy in the TSDC measurements and the different behavior of the MWS relaxation in the two temperature regions. In DSC measurements ordering and formation of a mesophase were observed only at high PDMS content, whereas the dielectric data suggest that this is the case for all the hybrid networks studied. This is explained by the different thermal history, in particular much lower cooling and heating rates in TSDC, as compared to DSC. The degree of ordering should depend on the PDMS content, which provides the explanation for the variation of the characteristics of TSDC MWS relaxation with composition (Table 2). Thus, the dielectric data on the MWS relaxation provide additional support for ordering and formation of a mesophase in the PDMS nanodomains at low temperatures.

A final comment on the MWS relaxation refers to the systematic shift of the DRS loss peak to lower frequencies with increasing PDMS content. A similar situation was observed in polystyrene-glass bead composites and explained quantitatively on the basis of the standard MWS formalism [27] by the fact that the conductivity of the matrix could not be ignored against that of the inclusions [31].

3.6. Water sorption isotherms

Fig. 9 shows the results of ESI measurements in pure PI at 298 K, which is also typical for the results obtained with the hybrid networks. The sorption data could not be fitted by a straight line, in agreement with results obtained in several PIs [32]. A linear increase of water content h with relative humidity RH would indicate that water is molecularly distributed in the PI film and does not form clusters. The sorption data in Fig. 9 and in the networks were analyzed by means of the GAB equation [14]

$$h = h_m \frac{cf\alpha}{(1 - f\alpha)[1 + (c - 1)f\alpha]} \quad (10)$$

In this equation, α is the water activity (= RH), h_m is the amount of water directly bound to the sorption sites (first monolayer sorption capacity), and c is the ratio of the binding constant of water molecules bound indirectly in the succeeding 'liquidlike' layers. f, in similar way, is the ratio of the standard chemical potential of the indirectly bound water molecules and of that of the free water molecules in the surrounding environment. The fittings were satisfactory. The maximum water uptake (at 97% RH) h_{max} and the first monolayer sorption capacity h_m were found to decrease linearly with increasing amount of PDMS in the networks (inset to Fig. 9). This result is consistent with reported negligible absorption of water in PDMS [33] and suggests a phase-separated morphology of the hybrid networks. Comparison of the sorption–desorption data in Fig. 9 and in the hybrid networks indicates that hysteresis effects are not very significant in the materials under investigation.

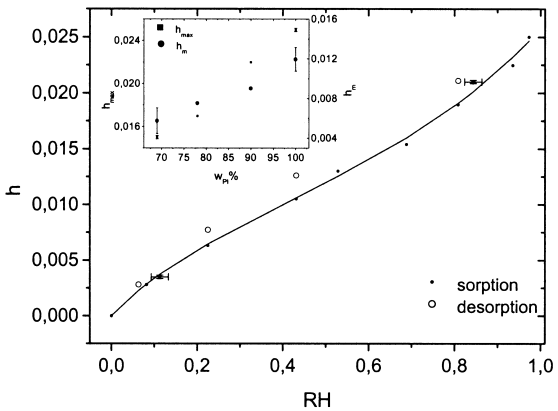

Fig. 9. Water content at equilibrium h versus relative humidity RH during sorption and desorption in pure PI. The line is a fit of the GAB equation to the experimental data. The inset shows the dependence of the maximum water content h_{max} and of the first monolayer capacity h_m on the weight fraction of PI w_{PI}. The errors shown in the figure correspond to the accuracy of measurements (RH, h, h_{max}) and to quality of the fits (h_m).

4. Conclusions

Dielectric techniques, including DRS and TSDC, and to a lesser extent DSC and water ESI, were employed to investigate molecular mobility in PI–PDMS hybrid networks. Besides their technological significance, the systems are also interesting from the fundamental point of view, as they allow to study the dynamics of short PDMS chains chemically bound to rigid PI at both ends.

The results suggest a microphase-separated morphology in the networks studied, in agreement with the results of NMR measurements on the same samples published recently. In particular, the results of water ESI and the dielectric results on the interfacial MWS relaxation support this conclusion. The maximum water uptake, obtained directly from the measurements, and the amount of water directly bound to the primary hydration sites, obtained by fitting of the GAB equation to the sorption data, were found to decrease linearly with increasing amount of PDMS content. The investigation of the MWS relaxation, on the other hand, provides information on characteristic properties of PDMS in the nanodomains, such as electrical conductivity, both at high temperatures, where PDMS is amorphous, and at lower temperatures, where some ordering and formation of a mesophase is observed.

In agreement with the microphase-separated morphology, T_g of the PI component was found to change only slightly with composition. It is, nevertheless, by about 30 °C lower than in pure PI, suggesting some interaction between the components. This is, however, by far less than in PI–PDMS block copolymers at the same composition. The magnitude of the local, secondary γ relaxation of PI, on the other hand, was found to increase considerably with increasing amount of PDMS, without any significant change of its time scale. Similar results have been obtained recently in hybrid PI/silica nanocomposites. They are explained as a result of loosened molecular packing of PI chains, as compared to pure PI, originating from the formation of chemical bonds with the PDMS nanodomains and from the geometrical confinement of PI in small volumes between these nanodomains. In agreement with this explanation, calculation of the distance between the PDMS particles, on the basis of some simplifying assumptions, give values in the range of 3–4 nm in the hybrid networks.

The glass transition temperature T_g of the PDMS component, determined by DSC, and the corresponding characteristic temperature of the α relaxation, obtained by DRS and TSDC, do not practically change with composition. The relaxation is observed by TSDC already at the lowest amount of PDMS studied, 10 wt%. The magnitude of the relaxation shows a complex dependence on the PDMS content, reflecting obviously the fact that the length of the PDMS chains, which affects drastically mobility at T_g, increases with the amount of PDMS. The time scale of the relaxation is very similar to that of the α relaxation in amorphous end-linked PDMS networks at comparable molecular weights between crosslinks. The broadening to both lower and higher temperature, observed by DSC in the glass transition region of PDMS in the hybrid networks, as compared to pure PDMS, is assigned to loosening of PDMS segmental packing and collapsing of intermolecular cooperativity due to nanoscale confinement and to some constraining influence of the rigid PI component on PDMS segmental motion. The same effects cause also suppression of crystallization of PDMS in the hybrid networks, so that only some ordering and formation of a mesophase are observed by DSC.

Acknowledgements

The authors are grateful to the programme ‘Thales’ (NTUA) and to the Russian Foundation for Basic Research (RFBR grant 00-03-33173) for the financial support of this research.

References

[1] Mittal KL, editor. Polyimides, vol. 1. New York: Plenum Press; 1984.
[2] Mittal KL, editor. Polyimides, vol. 2. New York: Plenum Press; 1984.
[3] Sroog CE. Prog Polym Sci 1991;16:561.
[4] Maier G. Prog Polym Sci 2001;26:3.
[5] Dvornic PR, Lenz RW. High temperature siloxane elastomers. Basel: Huthig and Wepf; 1990.
[6] Furukawa N, Yamada Y, Furukawa M, Yuasa M, Kimura Y. J Polym Sci Part A Polym Chem 1997;35:2239.
[7] McGrath JE, Dunson DL, Macham SJ, Hedrick JL. Adv Polym Sci 1999;140:61.
[8] Sysel P, Oupicky D. Polym Int 1996;40:275.
[9] Furukawa N, Yuasa M, Yamada Y, Kimura Y. Polymer 1998;39:2941.
[10] Sysel P, Hobzova R, Sindelar V, Brus J. Polymer 2001;42:10079.
[11] Brus J, Dybal J, Sysel P, Hobzova R. Macromolecules 2002;35:1253.
[12] Runt JP, Fitzgerald JJ, editors. Dielectric spectroscopy of polymeric materials. Washington, DC: American Chemical Society; 1997.
[13] Pissis P, Anagnostopoulou-Konsta A, Apekis L, Daoukaki-Diamanti D, Christodoulides C. J Non-Cryst Solids 1991;131–133:1174.
[14] Timmermann EO. J Chem Soc Faraday Trans 1 1989;85:1631.
[15] Schroeder MJ, Roland CM. Macromolecules 2002;35:2676.
[16] Kyritsis A, Pissis P, Mai S-M, Booth C. Macromolecules 2000;33:4581.
[17] Greenspan L. J Res Natl Bur Stand (US) 1977;81A:89.
[18] Bershtein VA, Egorova LM, Sysel P. J Macromol Sci Phys 1998;B37:747.
[19] Bershtein VA, Egorova LM, Yakushev PN, Pissis P, Sysel P, Brozova L. J Polym Sci Part B Polym Phys 2002;40:1056.
[20] Litvinov VM, Barthel H, Weis J. Macromolecules 2002;35:4356.
[21] Kirst KU, Kremer F, Litvinov VM. Macromolecules 1993;26:975.
[22] Bershtein VA, David L, Egorova LM, Kanapitsas A, Meszaros O, Pissis P, Sysel P, Yakushev PN. Mat Res Innovat 2002;5:230.
[23] Vatalis AS, Kanapitsas A, Delides CG, Pissis P. Thermochim Acta 2001;372:33.
[24] Pissis P, Kanapitsas A, Georgoussis G, Bershtein VA, Sysel P. Adv Compos Lett 2002;11:49.
[25] Mamunya YP, Davydenko VV, Pissis P, Lebedev EV. Eur Polym J 2002;38:1887.

[26] Donth E. Relaxation and thermodynamics in polymers. Glass transition. Berlin: Akademie; 1992.
[27] van Beek LKH. In: Birks JB, editor. Progress in dielectrics, vol. 7. London: Heywood; 1967. p. 69.
[28] Christodoulides C. J Phys D Appl Phys 1985;18:1501.
[29] Havriliak S, Negami S. J Polym Sci Polym Symp 1966;14:89.
[30] Hedvig P. Dielectric spectroscopy of polymers. Bristol: Adam Hilger; 1977.
[31] Perrier C, Bergeret A. J Polym Sci Part B Polym Phys 1997;35:1349.
[32] Okamoto K-I, Tanihara N, Watanabe H, Tanaka K, Kita H, Nakamura A, Kusuki Y, Nakagama K. J Polym Sci Polym Phys Ed 1992;30: 1223.
[33] Anderson JE, Adams KM. J Non-Cryst Solids 1991;131–133:587.